

Aligning the Band Gap of Graphene Nanoribbons by Monomer Doping**

Christopher Bronner,* Stephan Stremmlau, Marie Gille, Felix Brauße, Anton Haase, Stefan Hecht,* and Petra Tegeder*

Silicon-based field-effect transistors (FETs) are the building blocks of modern digital logic circuitry and therefore part of virtually every electronic device available today. Over the past decades, continuous downscaling of existing designs has met the rising performance requirements, but as the size of FETs approaches the regime of atomic structures, new concepts are required to maintain the current pace at which microelectronics is developing.^[1] At small gate channel lengths, the applicability of quantum mechanical principles results in several so-called short-channel effects (e.g. reduced carrier mobility).^[2] Since its experimental realization in 2004,^[3] graphene has been discussed intensively as a substitute for doped silicon in FETs because of its high charge carrier mobility and its unsurpassably low thickness.^[1,4] Graphene transistors have even been realized but cannot be put into the “off” state because of the lack of a band gap.^[5a,b] However, there are concepts available for opening a band gap, for example, applying strain^[6a,b] along the sheet or biasing bilayers of graphene.^[7a,b] Also, lateral confinement in quasi-one-dimensional graphene nanoribbons (GNRs) leads to a band gap, which furthermore is highly sensitive to the width and edge shape of the GNR, thus opening possibilities to tailor the electronic properties of a device.^[8a,b,c] Indeed, FETs built from nanoribbons show much higher on/off-ratios than graphene transistors, which makes them more suitable for integration into logic devices.^[9,10] However, the ability to control the electronic properties is essential: while the size of the gap can be engineered by varying the nanoribbon

widths,^[8c] the alignment of the GNR band structure with respect to the Fermi level of a metal electrode is equally important. Such a shifting of the entire band structure is observed both in two-dimensional graphene^[11] as well as in chemically synthesized or lithographically patterned GNRs^[12] upon doping, particularly with nitrogen atoms.^[13] Using present doping techniques, the distribution of dopant atoms will not be well-defined on the nanoscale and the band gap shift upon nitrogen doping depends on the site of the N atom, that is, the bonding configuration to neighboring carbon atoms.^[14] Generally, for doped and pristine GNRs, fabrication remains a challenge as well-established top-down approaches using lithography^[8c] or unzipping of carbon nanotubes^[15] yield relatively wide ribbons with an undetermined edge structure. Particularly for small widths on the order of a few nanometers (where the band gap reaches a technologically relevant size) atomically precise edges are necessary and can be realized using Br-substituted precursor molecules, which are thermally activated on a surface and—in a bottom-up synthesis—covalently assemble to a specific nanostructure.^[16a,b] In this study, we employed the latter approach to prepare GNRs with an atomically precise edge structure and doping pattern through polymerization of specific monomers directly on the Au(111) surface and studied the position and size of the band gap of these GNRs with surface-sensitive electron spectroscopies.

Besides straight armchair edge GNRs, another type of chevron-shaped nanoribbons has previously been fabricated using an on-surface reaction.^[16b] In this process adsorption of several layers of 6,11-dibromo-1,2,3,4-tetraphenyl-triphenylene (monomer **1** in Scheme 1) on Au(111) and heating at 250 °C leads to desorption of the second and higher layers as well as halogen dissociation and coupling of the resulting activated biradical monomers, yielding a sterically crowded and hence twisted polyphenylene. In a second heating step at 440 °C, this polymer undergoes a subsequent cyclodehydrogenation reaction providing access to the desired chevron-shaped GNR with armchair edges. Selective substitution of the parent monomer **1** with either one or two N atoms provided monomers **2** and **3**, respectively, which were used to generate GNRs with different doping levels (exemplarily shown for the doubly N doped GNR **5** in Scheme 1) and accordingly with potentially different electronic structure properties. Synthesis of the new monomers **2** and **3** was accomplished by Diels–Alder reactions of an appropriate cyclopentadienone with either mixed phenylpyridyl-acetylene or bispyridylacetylene, followed by immediate cheletropic CO extrusion (for details see the Supporting Information).

[*] C. Bronner, S. Stremmlau, A. Haase, Prof. Dr. P. Tegeder
Fachbereich Physik, Freie Universität Berlin
Arnimallee 14, 14195 Berlin (Germany)
E-mail: bronner@zedat.fu-berlin.de
petra.tegeder@physik.fu-berlin.de

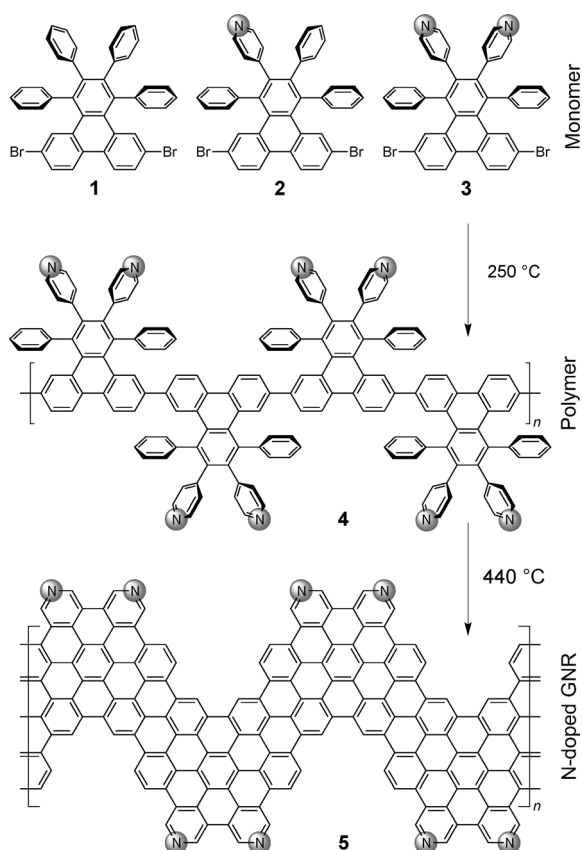
Dr. M. Gille, F. Brauße, Prof. Dr. S. Hecht
Department of Chemistry, Humboldt-Universität zu Berlin
Brook-Taylor-Straße 2, 12489 Berlin (Germany)
E-mail: sh@chemie.hu-berlin.de

Prof. Dr. P. Tegeder
Physikalisch-Chemisches Institut
Ruprecht-Karls-Universität Heidelberg
Im Neuenheimer Feld 253, 69120 Heidelberg (Germany)

[**] We gratefully acknowledge funding by the Focus Area Nanoscale at the Freie Universität Berlin, the German Research Foundation (DFG) through collaborative research center Sfb658, the European Union via the AtMol project, and the European Science Foundation via P2M. M.G. is indebted to the Fonds der chemischen Industrie for providing a Kekulé doctoral fellowship.



Supporting information for this article is available on the WWW under <http://dx.doi.org/10.1002/anie.201209735>.



Scheme 1. Monomers for the generation of graphene nanoribbons with defined edge-doping via on-surface polymerization followed by cyclo-dehydrogenation. Shown are monomers **1–3** with either none, one or two doping N-atoms, while the synthesis is exemplarily shown for the case of the doubly N-doped GNR.

After deposition of the monomers on the surface, we followed the two heating steps towards GNR formation using vibrational spectroscopy (Figure 1), namely angle-resolved high-resolution electron energy loss spectroscopy (HREELS) in analogy to a similar system.^[17] In the first heating step, the higher monomer layers are desorbed leading to an overall increase of the elastic peak (Figure 1b). Zero-order desorption, representative of multilayer desorption, is observed using a quadrupole mass spectrometer monitoring the C_6H_5Br fragment ion ($m/z = 158$ amu). Furthermore, the loss peak at 257 cm^{-1} , which we assign to the C–Br bending mode $\gamma(C-Br)$, vanishes because the Br atoms are detached from the molecule. The phenyl ring torsion mode $\tau(C-C)$ at 696 cm^{-1} and the out-of-plane bending mode $\gamma(C-H)$ at 798 cm^{-1} show a higher dipole activity mostly because in the first layer, the triphenylene moiety lies flat on the surface. A reduced dipole activity of the C–H stretching vibration $\nu(C-H)$ at 3063 cm^{-1} in the polymer phase results from a large portion of C–H bonds now pointing parallel to the surface. In the final GNR phase (Figure 1c), the torsion mode $\tau(C-C)$ is shifted to higher energies because of the changed environment within the more rigid graphene structure and the increased interaction with the substrate. The dipole activity of the out-of-plane bending mode $\gamma(C-H)$ is increased since all C–H bonds are lying parallel to the surface. The quenching of the various

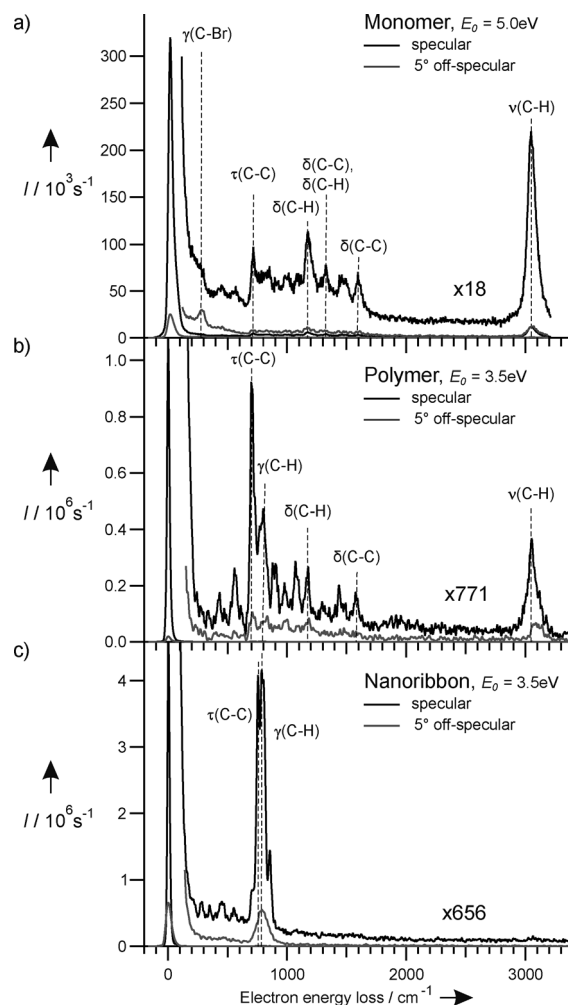


Figure 1. On-surface synthesis of the undoped GNR analyzed by vibrational HREELS in specular and off-specular scattering geometry for the three reaction steps: a) adsorbed monomers, b) polymer and c) graphene nanoribbon. E_0 is the primary energy of the incident electrons.

vibrational modes having dipole moments within the phenyl ring plane (including $\nu(C-H)$) is a consequence of all phenyl rings lying flat as part of the GNR. To estimate the GNR coverage after such a preparation temperature programmed desorption (TPD) experiments on co-adsorbed Xe were used (see the Supporting Information). From these studies, a GNR coverage of approximately 2/3 of a monolayer was determined. The preparation method as well as the characterization by means of HREELS and TPD were employed for all three monomers (**1–3**), giving similar results. Furthermore, the electronic HREELS (yielding electronic transition energies) signature changes drastically during both heating steps (see the Supporting Information).

Two complementary surface-sensitive spectroscopies were employed to study the electronic structure, that is, band gaps and energetic positions of the valence and conduction bands, of the differently doped GNRs. Electronic HREELS, which employs higher primary electron energies compared to the above shown vibrational HREELS, gives access to the width of the band gap by exciting electronic

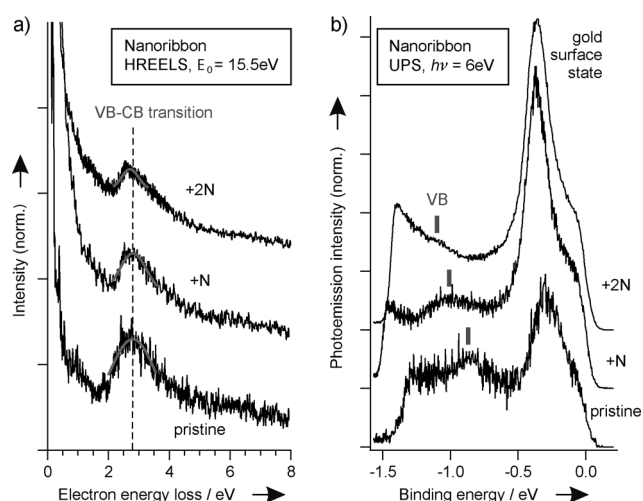


Figure 2. a) Electronic HREELS spectra for the three GNRs with different doping concentrations together with fits to the valence band (VB)–conduction band (CB) transition peak. The primary electron energy is 15.5 eV and the spectra are normalized with respect to the VB–CB transition peak. b) UPS spectra recorded with a photon energy of 6 eV showing the gold surface state and the valence band (VB) peak for all three GNRs. UPS spectra were normalized to the VB peak.

valence band (VB)–conduction band (CB) transitions. While electronic HREELS gives the size of the respective band gap, the alignment of the GNR band gap relative to the electronic structure of the underlying substrate is measured with ultraviolet photoelectron spectroscopy (UPS). Figure 2a shows electronic HREEL spectra for the pristine, undoped GNR produced from monomer **1** and the two doped monomers **2** and **3** in which the VB–CB transition peak has been fitted with Gaussian fit functions. The peak positions of the pristine GNR and the singly doped are identical, 2.80 ± 0.03 eV. The band gap of the doubly N-doped GNR (**5**) is slightly lower, 2.71 ± 0.01 eV, which corresponds to a reduction by 3%. UPS spectra recorded from the three different GNRs show two peaks: one at higher energies (i.e. closer to the Fermi level) that increases in intensity as more nitrogen atoms are present in the GNR, originates from the gold Shockley surface state. Its higher intensity relative to the other peak is indicative of decreasing coverages as we proceed to a higher doping level. Since the preparation was identical for all three systems, the varying coverage could be due to repulsive interactions among the electro-negative N atoms, favoring monomer desorption in the formation process compared to polymerization. The second peak originates from the GNR and exhibits an energy dependence on the degree of doping. Therefore, we assign the corresponding state to the valence band. Its binding energy in the pristine GNR is -0.87 ± 0.03 eV and decreases in the doped GNRs to -1.01 ± 0.03 eV (one N atom per molecule) and -1.10 ± 0.05 eV (two N atoms), respectively. Note that the downward shift in energy is in agreement with calculations^[14] and experiments on N-doped graphene^[11] as well as top-down fabricated graphene nanoribbons, the edge structure of which is not atomically precise.^[12] We thus observe a continuous downshifting of approximately 0.1 eV per N atom. Figure 3 sum-

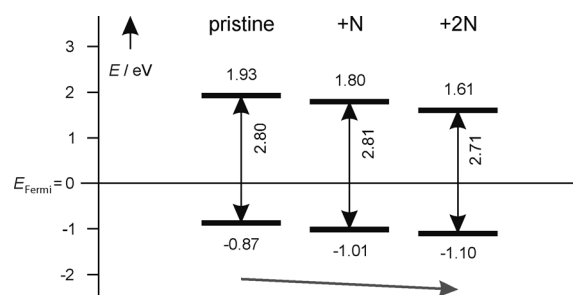


Figure 3. Summary of band gap size and alignment relative to the Fermi level of the gold substrate for the three investigated systems. While the band gap remains unaffected, the entire band structure is shifted toward lower energies.

marizes the energetic positions of the VB and CB of the studied GNRs.

In summary, we have successfully doped graphene nanoribbons in a well-defined manner by selective nitrogen substitution of the precursor monomers which does not interfere with the on-surface synthesis reaction. Using HREELS in combination with photoelectron spectroscopy, we could show that the band gap is linearly shifted relative to the electronic structure of the environment of the GNR but remains almost unchanged in magnitude, as expected for pyridine-like nitrogen at the edges of armchair GNRs.^[13] The positions of the bands and thus the size of the band gap agree well with other experimental data on the pristine GNR.^[18] The independence of the size of the band gap on one hand and its alignment relative to the Fermi level on the other hand could prove useful in tailoring the electronic properties of GNR devices. Doping the molecular precursors in a bottom-up fabrication technique furthermore allows a well-defined site selection and dosage of the dopant atoms within defect-free GNRs. This should add another powerful item to the toolbox of band gap engineering of graphene nanostructures and, together with width variation and edge shaping, thus contribute to controlling their properties towards technological applications.

Received: December 5, 2012

Revised: February 18, 2013

Published online: March 19, 2013

Keywords: doping · electronic structure · graphene · molecular electronics · surface chemistry

- [1] F. Schwierz, *Nat. Nanotechnol.* **2010**, *5*, 487–496.
- [2] R. Chau, B. Doyle, S. Datta, J. Kavalieros, K. Zhang, *Nat. Mater.* **2007**, *6*, 810–812.
- [3] K. S. Novoselov, A. K. Geim, S. V. Morozov, D. Jiang, Y. Zhang, S. V. Dubonos, I. V. Grigorieva, A. A. Firsov, *Science* **2004**, *306*, 666–669.
- [4] K. S. Novoselov, A. K. Geim, S. V. Morozov, D. Jiang, M. I. Katsnelson, I. V. Grigorieva, S. V. Dubonos, A. A. Firsov, *Nature* **2005**, *438*, 197–200.
- [5] a) I. Meric, M. Y. Han, A. F. Young, B. Ozyilmaz, P. Kim, K. L. Shepard, *Nat. Nanotechnol.* **2008**, *3*, 654–659; b) F. Xia, D. B. Farmer, Y.-M. Lin, P. Avouris, *Nano Lett.* **2010**, *10*, 715–718.

- [6] a) Z. H. Ni, T. Yu, Y. H. Lu, Y. Y. Wang, Y. P. Feng, Z. X. Shen, *ACS Nano* **2008**, *2*, 2301–2305; b) T. M. G. Mohiuddin, A. Lombardo, R. R. Nair, et al., *Phys. Rev. B* **2009**, *79*, 205433.
- [7] a) Y. Zhang, T.-T. Tang, C. Girit, Z. Hao, M. C. Martin, A. Zettl, M. F. Crommie, Y. R. Shen, F. Wang, *Nature* **2009**, *459*, 820–823; b) T. Ohta, A. Bostwick, T. Seyller, K. Horn, E. Rotenberg, *Science* **2006**, *313*, 951–954.
- [8] a) K. Nakada, M. Fujita, G. Dresselhaus, M. S. Dresselhaus, *Phys. Rev. B* **1996**, *54*, 17954–17961; b) Y.-W. Son, M. L. Cohen, S. G. Louie, *Phys. Rev. Lett.* **2006**, *97*, 216803; c) M. Y. Han, B. Özyilmaz, Y. Zhang, P. Kim, *Phys. Rev. Lett.* **2007**, *98*, 206805.
- [9] X. Li, X. Wang, L. Zhang, S. Lee, H. Dai, *Science* **2008**, *319*, 1229–1232.
- [10] X. Wang, Y. Ouyang, X. Li, H. Wang, J. Guo, H. Dai, *Phys. Rev. Lett.* **2008**, *100*, 206803.
- [11] a) D. Wei, Y. Liu, Y. Wang, H. Zhang, L. Huang, G. Yu, *Nano Lett.* **2009**, *9*, 1752–1758; b) H. Wang, T. Maiyalagan, X. Wang, *ACS Catal.* **2012**, *2*, 781–794.
- [12] X. Wang, X. Li, L. Zhang, Y. Yoon, P. K. Weber, H. Wang, J. Guo, H. Dai, *Science* **2009**, *324*, 768–771.
- [13] H. Terrones, R. Lv, M. Terrones, M. S. Dresselhaus, *Rep. Prog. Phys.* **2012**, *75*, 062501.
- [14] F. Cervantes-Sodi, G. Csányi, S. Piscanec, A. C. Ferrari, *Phys. Rev. B* **2008**, *77*, 165427.
- [15] D. V. Kosynkin, A. L. Higginbotham, A. Sinitskii, J. R. Lomeda, A. Dimiev, B. K. Price, J. M. Tour, *Nature* **2009**, *458*, 872–876.
- [16] a) L. Grill, M. Dyer, L. Lafferentz, M. Persson, M. V. Peters, S. Hecht, *Nat. Nanotechnol.* **2007**, *2*, 687–691; b) J. Cai, P. Ruffieux, R. Jaafar, M. Bieri, T. Braun, S. Blankenburg, M. Muoth, A. P. Seitsonen, M. Saleh, X. Feng, K. Müllen, R. Fasel, *Nature* **2010**, *466*, 470–473.
- [17] C. Bronner, F. Leyssner, S. Stremlau, M. Utecht, P. Saalfrank, T. Klamroth, P. Tegeder, *Phys. Rev. B* **2012**, *86*, 085444.
- [18] S. Linden, D. Zhong, A. Timmer, N. Aghdassi, J. H. Franke, H. Zhang, X. Feng, K. Müllen, H. Fuchs, L. Chi, H. Zacharias, *Phys. Rev. Lett.* **2012**, *108*, 216801.